Acta Crystallographica Section C
Crystal Structure Communications
ISSN 0108-2701

Two new structures in the glycine–oxalic acid system

Nikolay A. Tumanov,[a]* Elena V. Boldyreva[a,b] and Natalia E. Shikina[a,b]

[a]REC-008, Novosibirsk State University, Pirogova 2, Novosibirsk 630090, Russian Federation, and [b]Institute of Solid State Chemistry and Mechanochemistry, Siberian Branch of the Russian Academy of Sciences, Kutateladze 18, Novosibirsk 630128, Russian Federation
Correspondence e-mail: n.tumanov@gmail.com

Received 3 February 2010
Accepted 27 April 2010
Online 8 May 2010

Glycinium semi-oxalate-II, $C_2H_6NO_2^+\cdot C_2HO_4^-$, (*A*), and diglycinium oxalate methanol disolvate, $2C_2H_6NO_2^+\cdot C_2O_4^{2-}\cdot 2CH_3OH$, (*B*), are new examples in the glycine–oxalic acid family. (*A*) is a new polymorph of the known glycinium semi-oxalate salt, (*C*). Compounds (*A*) and (*C*) have a similar packing of the semi-oxalate monoanions with respect to the glycinium cations, but in (*A*) the two glycinium cations and the two semi-oxalate anions in the asymmetric unit are non-equivalent, and the binding of the glycinium cations to each other is radically different. Based on this difference, one can expect that, although the two forms grow concomitantly from the same batch, a transformation between (*A*) and (*C*) in the solid state should be difficult. In (*B*), two glycinium cations and an oxalate anion, which sits across a centre of inversion, are linked *via* strong short O—H···O hydrogen bonds to form the main structural fragment, similar to that in diglycinium oxalate, (*D*). Methanol solvent molecules are embedded between the glycinium cations of neighbouring fragments. These fragments form a three-dimensional network *via* N—H···O hydrogen bonds. Salts (*B*) and (*D*) can be obtained from the same solution by, respectively, slow or rapid antisolvent crystallization.

Comment

Amino acids attract attention as drugs, biomimetics and molecular materials (Boldyreva, 2007). They are interesting as a structural element for forming complexes with carboxylic acids: the amino and carboxylic acid groups, and in many cases also the side chains, are capable of forming hydrogen bonds with the carboxyl groups of the carboxylic acids, giving rise to a variety of crystal structures. The main structural elements which are found in the pure forms of amino acids (*e.g.* head-to-tail chains) may or may not be preserved when introducing additional species into the structure.

Glycine is the simplest amino acid and an optically inactive one, but it gives rise to multiple polymorphs as an individual compound, and to a rich variety of crystalline salts. Recently, the crystal structures of salts formed by glycine and oxalic acid have been described, namely glycinium semi-oxalate, (*C*) (Subha Nandhini *et al.*, 2001), and diglycinium oxalate, (*D*) (Chitra *et al.*, 2006; Chitra & Choudhury, 2007). The present contribution reports the structures of two new compounds from the same family, a new polymorph of glycinium semi-oxalate, (*A*), and diglycinium oxalate methanol disolvate, (*B*).

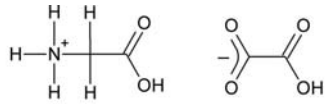

(*A*)

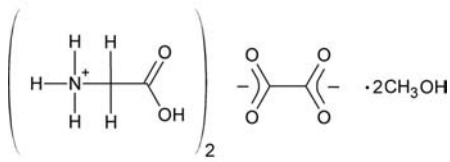

(*B*)

The asymmetric unit of (*A*) contains two symmetry-independent pairs of glycinium cations, NH_3^+–CH_2–COOH, and semi-oxalate anions, HCOO–COO^- (Z' = 2) (Fig. 1), the backbone conformations of which differ significantly (compare the torsion angles in Table 2). In (*A*), the semi-oxalate anions are linked *via* O—H···O hydrogen bonds into stacked chains of alternating symmetrically non-equivalent anions. Strictly speaking, these chains can be described by a $C_2^2(10)$ motif (Bernstein, 2002), since the chain has two independent oxalate ions. However, it could be approximated as $C(5)$, if the difference between the non-equivalent oxalates is neglected. The chains are similar to the arrangement in salt (*C*), but, in contrast with (*C*), where the chains are planar, the chains in (*A*) have the form of a gently undulating wave which propagates in the [201] direction (Figs. 2*b* and 3*a*). The O···O

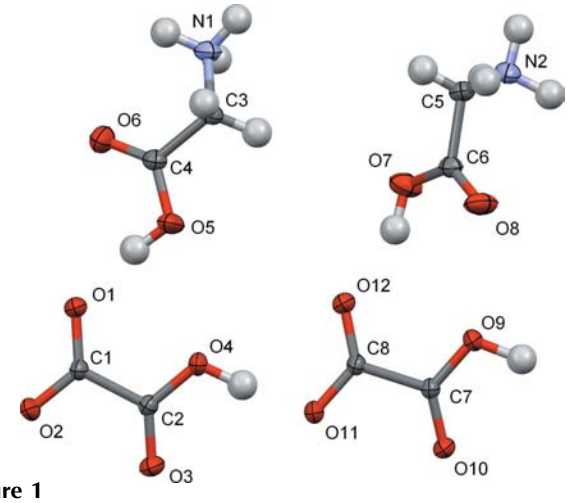

Figure 1
A displacement ellipsoid plot of glycinium semi-oxalate, (*A*), showing the atom-numbering scheme and 50% probability displacement ellipsoids. H atoms are shown as arbitrary spheres.

 doi:10.1107/S0108270110015519

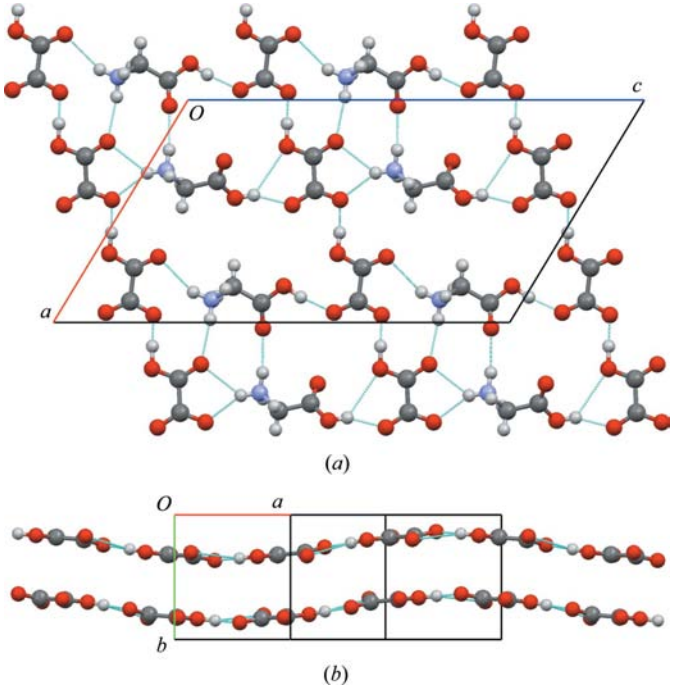

Figure 2
(*a*) The structure of the (010) layer in (*A*). One can see chains of semi-oxalate anions along [201], and chains of alternating glycinium cations and semi-oxalate anions along [001]. (*b*) Undulating chains of semi-oxalate anions, viewed along [20$\bar{1}$]. Glycinium cations have been omitted for clarity. Hydrogen bonds are shown as dashed lines.

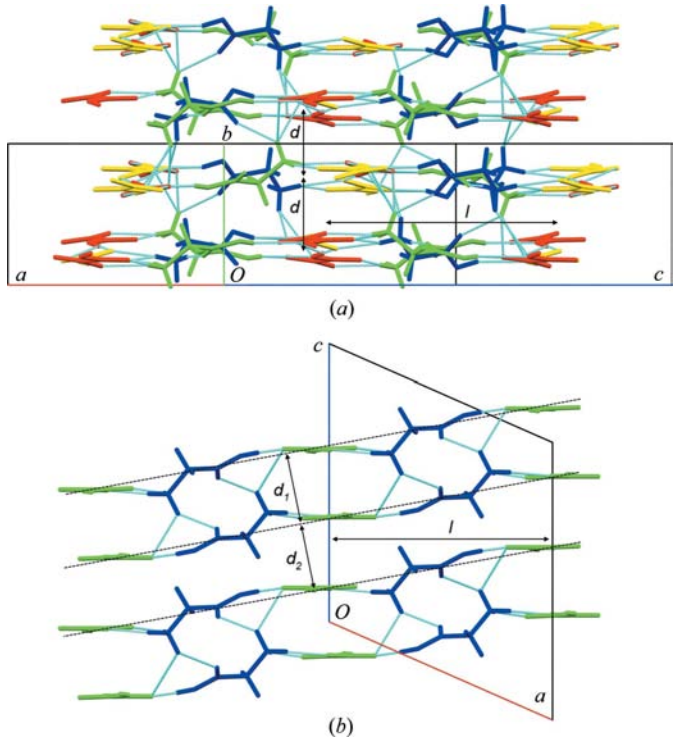

Figure 3
A comparison of the packing in the two semi-oxalate polymorphs, *viz.* (*a*) (*A*) and (*b*) (*C*), viewed along the direction of the semi-oxalate ribbons. Molecules are coloured by symmetry equivalence. The distances *l*, *d*, d_1 and d_2 are discussed in the *Comment*. Hydrogen bonds are shown as dashed lines.

distances between semi-oxalate anions in (*A*) are shorter than those in (*C*) (Table 2). The chains of semi-oxalate anions are linked to each other *via* glycinium bridges, forming N—H···O and O—H···O hydrogen bonds [these bonds form $C_2^2(9)$ and $C_2^2(10)$ chains along the [001] direction] with semi-oxalate anions, giving a slightly folded layer which lies parallel to the (010) plane (Fig. 2*a*). These layers are further connected to each other *via* a cluster of four glycinium cations, two symmetry-independent cations from each layer, which are linked by head-to-tail N—H···O hydrogen bonds to give an $R_4^4(20)$ motif, thereby completing a three-dimensional network (Table 1). The glycinium cations in (*A*) do not form head-to-tail chains, neither planar (as in all the polymorphs of glycine) nor helical [as in (*C*)].

Polymorph-I and -II have a similar packing of the semi-oxalate anions with respect to the glycinium cations (Fig. 3). The semi-oxalate chains are directed along [201] in (*A*), and along [010] in (*C*). The stacking directions also differ with respect to the crystallographic axes. At the same time, the distances between the molecules within a chain are similar in the two polymorphs: in (*A*) the period of a chain including four semi-oxalate anions is 22.033 (2) Å, whereas in (*C*) four periods of a chain including one semi-oxalate anion each are equal to 22.600 (6) Å. The distances between all the neighbouring chains in an undulating stack in (*A*) are the same (defined as *d* in Fig. 3*a*), whereas in (*C*) two non-equivalent distances alternate (defined as d_1 and d_2 in Fig. 3*b*). However, 2*d* in (*A*) is close to the sum of d_1 and d_2 in (*C*) [5.6481 (6) and 5.948 (2) Å, respectively]. In both (*A*) and (*C*), stacks of semi-oxalate anions alternate with columns formed by glycinium cations, and the distances between the semi-oxalate stacks, *l*, are very similar: 9.6000 (8) Å in (*A*) and 9.679 (2) Å in (*C*) (Fig. 3). At the same time, the binding of the glycinium cations to each other is radically different in (*A*) compared with (*C*). In (*C*), the helical chains of glycinium cations are linked *via* N—H···O hydrogen bonds connecting the individual layers, and this makes d_1 shorter than d_2 and forms a structure consisting of double layers. All the glycinium cations within one individual layer have the same orientation. In (*A*), the orientation of the glycinium cations is different within a layer, and the layers are linked not *via* glycinium cations only, but *via* a more complex hydrogen-bond pattern involving the N—H···O hydrogen bonds between glycinium cations and semi-oxalate anions, so that a three-dimensional network is formed (Fig. 3). Based on this difference, one can expect that, although the two forms grow concomitantly from the same batch, a transformation between the two structures in the solid state should be difficult.

Both (*A*) and (*C*) have structural elements similar to those in the structures of the individual oxalic acid and glycine molecules. The packing of the semi-oxalate anions (hydrogen-bonded chains) is quite common for oxalate-containing crystal structures, as is the formation of stacks. The way the helical chains of glycinium cations are linked to each other in (*C*) can be compared with the formation of centrosymmetric dimers in α-glycine. The four-membered clusters [$R_4^4(20)$ hydrogen-

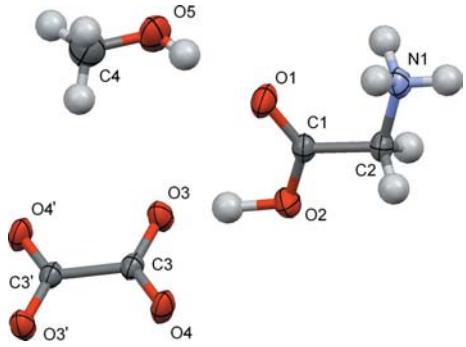

Figure 4
A displacement ellipsoid plot of diglycinium oxalate methanol disolvate, (*B*), showing the atom-numbering scheme and 50% probability displacement ellipsoids. H atoms are shown as arbitrary spheres. [Symmetry code: (i) $-x+1, -y+1, -z+1$.]

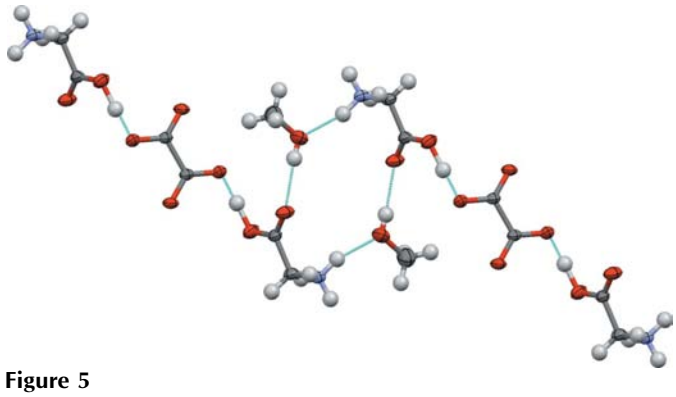

Figure 5
Two fragments of the diglycinium oxalate methanol disolvate structure, showing the formation of hydrogen-bonded ribbons. Methanol solvent molecules are embedded between glycinium cations, preventing the formation of glycinium dimers. At the centre, one can see the $R_4^4(14)$ *cdcd* motif, which includes methanol molecules. Hydrogen bonds are shown as dashed lines.

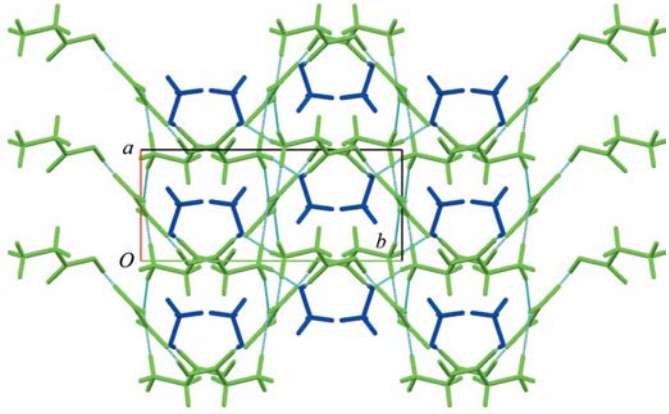

Figure 6
The crystal packing in (*B*), viewed along the *c* axis. Hydrogen bonds are shown as dashed lines. In the electronic version of the paper, glycinium cations and oxalate anions are coloured green (light) and methanol molecules are coloured blue (dark).

bond motif] of glycinium cations in (*A*) resemble those in α-glycine (Bernstein & Davis, 1999). One can suppose that the two polymorphic structures of the same salt, (*A*) and (*C*), reflect the structures of clusters simultaneously present in aqueous solutions containing glycine and oxalic acid, and that the direction of the crystallization into different polymorphs depends on the structure of the 'primary nuclei'. This hypothesis is within the approach suggested, for example, in the early work by Leonidov and co-workers (Leonidov, 1997; Leonidov *et al.*, 1994, 1993) and presently developed by several research groups and summarized by Gavezzotti (2007).

The asymmetric unit of (*B*) contains a glycinium cation, half of an oxalate anion, which sits across a centre of inversion, and a methanol solvent molecule (Fig. 4). With the exception of the methanol molecule, the chemical formula is essentially the same as in (*D*). The oxalate anions are planar in both forms. The non-equivalence of the oxalate C—O bonds is apparently a consequence of the formation of a very short O—H···O hydrogen bond with the glycinium cation: the shorter C—O bond [1.2381 (14) Å] corresponds to atom O4, which accepts two longer hydrogen bonds, and the longer one [1.2684 (16) Å] corresponds to the O atom which acts as the acceptor of the short O—H···O interaction (Fig. 5). The calculated contoured difference Fourier maps in the planes of all the C—O—H groups (cations and anions) in which the H atom has been omitted from the structure-factor calculations suggest that, for both structures (*B*) and (*D*), the electron density is smeared between the oxalates. The short O—H···O bonds are not symmetric, and the values of the N—C—C—O torsion angles of the glycinium cations in (*B*) and (*D*) differ (Table 4). Although oxalate anions are often planar in crystal structures, quantum chemical calculations have shown that a 'free' oxalate anion should be twisted, and it is the interaction with the crystalline environment (the requirements of more efficient packing, chelating cations and formation of hydrogen bonds) that accounts for the planarity of the oxalate anion in a crystal structure (Naumov *et al.*, 1997).

Salts (*B*) and (*D*) crystallize in the same space group, $P2_1/c$, with similar unit-cell parameters [the values for (*D*) are a = 4.9199 (18) Å, b = 9.959 (4) Å and c = 11.320 (4) Å, and β = 108.010 (3)°; the choice of the unit cell is altered compared with that of Chitra *et al.* (2006), to obtain the standard space group setting $P2_1/c$]. The crystal structure of (*B*) is, in general, very similar to that of (*D*). In both structures, an oxalate anion and two glycinium cations form a similar centrosymmetric fragment *via* very short O—H···O hydrogen bonds. These fragments form stacks (Fig. 6). In (*D*), the glycinium cations form hydrogen-bonded dimers, which link these fragments to each other. In (*B*), the methanol solvent molecules are embedded between such pairs of glycinium cations *via* O—H···O and N—H···O hydrogen bonds, connecting fragments to each other to form infinite ribbons which run parallel to the [1$\bar{1}$0] and [110] directions. Ribbons with different orientations are linked *via* N—H···O hydrogen bonds between the NH_3 group of the glycinium cation of one fragment and the oxalate anion of the other. Each NH_3 group is connected to two fragments, thus forming a three-dimensional hydrogen-bond network (Fig. 6 and Table 3).

A comparative analysis of the graph sets describing the hydrogen-bond networks in (*B*) and (*D*) can be significantly simplified if the short O2—H2···O3 hydrogen bond is treated as if it were intramolecular. Part of the first-level graph sets of (*B*), which corresponds to hydrogen bonds *a* and *b* in Table 3 [*C*(9) *a*, *C*(9) *b*, *C*(10) *a*, *C*(10) *b*, $R_4^4(38)$ *aaaa* and $R_4^4(38)$ *bbbb*], is in common with the graph sets of (*D*). These hydrogen bonds connect ribbons with different orientations. Other first-level graph sets present in (*D*), namely *C*(14), $R_2^2(10)$ and $C_2^2(28)$, correspond to hydrogen bonds linking the glycinium cations into dimers. Because of the embedded methanol, in (*B*) these graph sets are transformed into the second-level graph sets $C_2^2(16)$ *cd*, $R_4^4(14)$ *cdcd* (shown in Fig. 5) and $C_4^4(32)$ *cdcd*, respectively.

The solvate (*B*) is metastable and when stored in air transforms into (*D*), as has been confirmed by X-ray powder diffraction analysis. During this transition, a single crystal transforms into a polycrystalline pseudomorph, preserving the crystal habit.

The crystal structures of (*B*) and (*D*) illustrate that minor modifications to the crystallization procedure from the same solution can result in a new manner of self-assembly of the same species to give a new crystalline form. The two forms can be obtained from an aqueous solution containing glycine and oxalic acid by adding methanol. If methanol is added slowly and the crystals grow on evaporation of the solution, methanol molecules become embedded between the glycinium cations and are preserved in the crystal structure. If the same solution is stirred to trigger a rapid antisolvent crystallization, the glycinium cations form dimers and methanol is no longer present in the final crystal structure.

Experimental

Crystals of (*A*) were obtained by slow evaporation from a saturated aqueous solution of glycine and oxalic acid in a 1:1 stoichiometric ratio. Colourless needle-shaped crystals of (*A*) were grown from the same crystallization batch as plate-shaped crystals of the known polymorph of glycine oxalate, (*C*). Interestingly, polymorph (*A*) could not be obtained on co-grinding of oxalic acid dihydrate and glycine, in contrast with polymorph (*C*).

Colourless needle-shaped crystals of (*B*) were obtained from aqueous solutions with variable ratios of the initial components (1:1 or 2:1 glycine–oxalic acid) using methanol as an antisolvent, if the solution was not stirred or disturbed in any other way. The volume of added methanol was approximately equal to the volume of the initial saturated aqueous solution. Interestingly, if the same amount of methanol was added rapidly to the same solution with energetic stirring, a powder sample of diglycinium oxalate, (*D*), was formed.

Compound (*A*)

Crystal data

$C_2H_6NO_2^+\cdot C_2HO_4^-$
M_r = 165.11
Monoclinic, $P2_1/c$
a = 11.8719 (8) Å
b = 6.1493 (2) Å
c = 20.8247 (14) Å
β = 121.180 (5)°
V = 1300.67 (15) Å^3
Z = 8
Mo $K\alpha$ radiation
μ = 0.16 mm^{-1}
T = 300 K
0.5 × 0.36 × 0.22 mm

Table 1
Hydrogen-bond geometry (Å, °) for (*A*).

D—H···*A*	*D*—H	H···*A*	*D*···*A*	*D*—H···*A*
O4—H4···O11	0.97 (3)	1.53 (3)	2.4972 (12)	175 (2)
O5—H5···O1	0.92 (2)	1.68 (2)	2.5923 (13)	171 (2)
O7—H7···O12	0.91 (3)	1.81 (3)	2.6586 (14)	153 (2)
O9—H9···O2^{i}	1.04 (3)	1.44 (3)	2.4744 (12)	178 (3)
N1—H11···O10^{ii}	0.92 (2)	2.10 (3)	3.0128 (15)	171 (2)
N1—H12···O8^{iii}	0.87 (3)	2.24 (2)	2.8800 (16)	131 (2)
N1—H12···O1^{iv}	0.87 (3)	2.50 (2)	3.1259 (17)	129.4 (18)
N1—H13···O2^{v}	0.91 (2)	2.09 (2)	2.7476 (14)	128.2 (19)
N1—H13···O3^{v}	0.91 (2)	2.28 (2)	3.1340 (15)	157 (2)
N2—H21···O6^{i}	0.95 (2)	2.03 (2)	2.9626 (16)	169 (2)
N2—H22···O10^{v}	0.89 (2)	2.32 (2)	2.9854 (14)	131.8 (16)
N2—H22···O11^{v}	0.89 (2)	2.04 (2)	2.8510 (14)	150.7 (17)
N2—H23···O12^{vi}	0.91 (2)	2.28 (2)	3.0476 (16)	141.9 (17)

Symmetry codes: (i) $x-1, -y+\frac{1}{2}, z-\frac{1}{2}$; (ii) $x+1, y, z$; (iii) $-x+1, y+\frac{1}{2}, -z+\frac{1}{2}$; (iv) $-x+2, -y+1, -z+1$; (v) $x, -y+\frac{1}{2}, z-\frac{1}{2}$; (vi) $-x+1, y-\frac{1}{2}, -z+\frac{1}{2}$.

Table 2
A comparison of selected torsion angles (°) and interatomic distances (Å) for the hydrogen bonds in the glycinium semi-oxalate polymorphs (*A*) and (*C*).

Parameter	*A*	*C*^{a}
O···O†	2.4756 (13) 2.4991 (12)	2.540 (2)
O—C—C—O‡	29.00 (18) 6.59 (17)	3.57 (18)
N—C—C—O	9.85 (15) 6.76 (16)	24.7 (2)

† The O···O distance in semi-oxalate anion chains. ‡ The smallest positive torsion angle in semi-oxalate anions, which involves an O atom connected to an H atom. Reference: (*a*) Subha Nandhini *et al.* (2001) at 293 K.

Data collection

Stoe IPDS II diffractometer
Absorption correction: multi-scan (Blessing, 1995)
T_{min} = 0.930, T_{max} = 0.965
11921 measured reflections
3518 independent reflections
3035 reflections with $I > 2\sigma(I)$
R_{int} = 0.036

Refinement

$R[F^2 > 2\sigma(F^2)]$ = 0.047
$wR(F^2)$ = 0.119
S = 1.07
3518 reflections
255 parameters
All H-atom parameters refined
$\Delta\rho_{max}$ = 0.31 e Å^{-3}
$\Delta\rho_{min}$ = −0.36 e Å^{-3}

Compound (*B*)

Crystal data

$2C_2H_6NO_2^+\cdot C_2O_4^{2-}\cdot 2CH_4O$
M_r = 304.26
Monoclinic, $P2_1/c$
a = 5.0068 (7) Å
b = 11.3293 (15) Å
c = 12.893 (2) Å
β = 106.077 (12)°
V = 702.72 (17) Å^3
Z = 2
Mo $K\alpha$ radiation
μ = 0.13 mm^{-1}
T = 295 K
0.7 × 0.35 × 0.3 mm

Data collection

Stoe IPDS II diffractometer
Absorption correction: multi-scan (Blessing, 1995)
T_{min} = 0.917, T_{max} = 0.962
6655 measured reflections
1889 independent reflections
1423 reflections with $I > 2\sigma(I)$
R_{int} = 0.055

Refinement

$R[F^2 > 2\sigma(F^2)] = 0.042$	H atoms treated by a mixture of independent and constrained refinement
$wR(F^2) = 0.111$	$\Delta\rho_{max} = 0.27$ e Å^{-3}
$S = 1.06$	$\Delta\rho_{min} = -0.24$ e Å^{-3}
1889 reflections	
120 parameters	

Table 3
Hydrogen-bond geometry (Å, °) for (*B*).

	D—H···*A*	*D*—H	H···*A*	*D*···*A*	*D*—H···*A*
	O2—H2···O3	1.16 (3)	1.31 (3)	2.4656 (12)	177 (3)
d	O5—H5···O1	0.79 (3)	2.03 (3)	2.8102 (15)	176 (2)
c	N1—H11···O5^{i}	0.951 (18)	1.863 (19)	2.7844 (16)	162.4 (16)
a	N1—H12···O4^{ii}	0.90 (2)	2.01 (2)	2.9020 (17)	178.7 (18)
b	N1—H13···O4^{iii}	0.91 (2)	1.97 (2)	2.8695 (14)	166.8 (17)

Symmetry codes: (i) $-x, -y, -z+1$; (ii) $-x+1, y-\frac{1}{2}, -z+\frac{3}{2}$; (iii) $-x, y-\frac{1}{2}, -z+\frac{3}{2}$.

Table 4
A comparison of selected torsion angles (°) and interatomic distances (Å) for the hydrogen bonds in diglycinium oxalate, (*D*), and diglycinium oxalate methanol disolvate, (*B*).

Parameter	(II)	(IV)^{a,b}
O···O†	2.4656 (12)	2.4544 (15)/2.461 (5)
N—C—C—O	0.60 (18)	16.2 (2)/15.5 (3)

† The distance between the glycinium cation and oxalate anion. References: (*a*) Chitra *et al.* (2006) (X-ray single-crystal diffraction at 300 K); (*b*) Chitra & Choudhury (2007) (neutron single-crystal diffraction at 300 K).

All H atoms were located in difference Fourier maps. H atoms bonded to the methanol C atom in (*B*) were treated as riding atoms in geometrically idealized positions, with C—H = 0.96 Å and U_{iso}(H) = 1.5U_{eq}(C). The methyl group was permitted to rotate but not to tilt. The positions and isotropic displacement parameters of all other H atoms were refined freely.

For both compounds, data collection: *X-AREA* (Stoe & Cie, 2006); cell refinement: *X-AREA*; data reduction: *X-RED* (Stoe & Cie, 2006); program(s) used to solve structure: *SHELXS97* (Sheldrick, 2008) and *X-STEP32* (Stoe & Cie, 2000); program(s) used to refine structure: *SHELXL97* (Sheldrick, 2008) and *X-STEP32*; molecular graphics: *Mercury* (Macrae *et al.*, 2006); software used to prepare material for publication: *Mercury*, *PLATON* (Spek, 2009), *publCIF* (Westrip, 2010) and *enCIFer* (Allen *et al.*, 2004).

This work was supported by grants from BRHE (grant No. RUX0-008-NO-06) and RFBR (grant No. 09-03-00451), by Integration Projects Nos. 13 and 109 of the Siberian Branch of the Russian Academy of Sciences, by project Nos. 27.44 and 5.6.4 of the Presidium of the Russian Academy of Sciences, and by a FASI grant (No. P2529). The diffractometer was purchased with financial support from the Innovation Project Education (No. 456) from the Russian Ministry of Science and Education.

Supplementary data for this paper are available from the IUCr electronic archives (Reference: LN3139). Services for accessing these data are described at the back of the journal.

References

Allen, F. H., Johnson, O., Shields, G. P., Smith, B. R. & Towler, M. (2004). *J. Appl. Cryst.* **37**, 335–338.
Bernstein, J. (2002). In *Polymorphism in Molecular Crystals*. Oxford University Press.
Bernstein, J. & Davis, R. E. (1999). *Implications of Molecular and Materials Structure for New Technologies*, edited by J. A. K. Howard, F. H. Allen & G. P. Shields, pp. 275–290. Dordrecht: Kluwer Academic Publishers.
Blessing, R. H. (1995). *Acta Cryst.* A**51**, 33–38.
Boldyreva, E. V. (2007). *Models, Mysteries and Magic of Molecules*, edited by J. C. A. Boeyens & J. F. Ogilvie, pp. 169–194. Dordrecht: Springer Verlag
Chitra, R. & Choudhury, R. R. (2007). *Acta Cryst.* B**63**, 497–504.
Chitra, R., Thiruvenkatam, V., Choudhury, R. R., Hosur, M. V. & Guru Row, T. N. (2006). *Acta Cryst.* C**62**, o274–o276.
Gavezzotti, A. (2007). In *Molecular Aggregation*. Oxford University Press.
Leonidov, N. B. (1997). *Russ. Chem. J.* **41**(5), 22–23.
Leonidov, N. B., Uspenskaya, S. I., Tolmachev, A. M., Juravlev, V. I., Korableva, E. Yu. & Usacheva, T. M. (1994). *Russ. J. Phys. Chem.* **68**, 890–894.
Leonidov, N. B., Zorky, P. M., Masunov, A. E., Gladkih, O. P., Belskih, V. K., Dzyabchenko, A. V. & Ivanov, C. A. (1993). *Russ. J. Phys. Chem.* **67**, 2464–2468.
Macrae, C. F., Edgington, P. R., McCabe, P., Pidcock, E., Shields, G. P., Taylor, R., Towler, M. & van de Streek, J. (2006). *J. Appl. Cryst.* **39**, 453–457.
Naumov, D. Yu., Boldyreva, E. V., Howard, J. A. K. & Podberezskaya, N. V. (1997). *Solid State Ionics*, **101–103**, 1315–1320.
Sheldrick, G. M. (2008). *Acta Cryst.* A**64**, 112–122.
Spek, A. L. (2009). *Acta Cryst.* D**65**, 148–155.
Stoe & Cie (2000). *X-STEP32*. Stoe & Cie, Darmstadt, Germany.
Stoe & Cie (2006). *X-AREA* and *X-RED32*. Stoe & Cie, Darmstadt, Germany.
Subha Nandhini, M., Krishnakumar, R. V. & Natarajan, S. (2001). *Acta Cryst.* C**57**, 115–116.
Westrip, S. P. (2010). *J. Appl. Cryst.* **43**. Submitted.